

Numerical investigation of glass windows under near-field blast

Chiara Bedon^{*1}, Damijan Markovic^{2a}, Vasilis Karlos^{2b} and Martin Larcher^{2c}

¹Department of Engineering and Architecture, University of Trieste, 34172 Trieste, Italy

²European Commission, Joint Research Centre, 21027 Ispra, VA, Italy

(Received March 28, 2023, Revised April 29, 2023, Accepted April 30, 2023)

Abstract. The determination of the blast protection level and the corresponding minimum load-bearing capacity for a laminated glass (LG) window is of crucial importance for safety and security design purposes. In this paper, the focus is given to the window response under near-field blast loading, i.e., where relatively small explosives would be activated close to the target, representative of attack scenarios using small commercial drones. In general, the assessment of the load-bearing capacity of a window is based on complex and expensive experiments, which can be conducted for a small number of configurations. On the other hand, nowadays, validated numerical simulation tools based on the Finite Element Method (FEM) are available to partially substitute the physical tests for the assessment of the performance of various LG systems, especially for the far-field blast loading. However, very little literature is available on the LG window performance under near-field blast loads, which differs from far-field situations in two points: i) the duration of the load is very short, since the blast wavelength tends to increase with the distance and ii) the load distribution is not uniform over the window surface, as opposed to the almost plane wave configuration for far-field configurations. Therefore, the current study focuses on the performance assessment and structural behaviour of LG windows under near-field blasts. Typical behavioural trends are investigated, by taking into account possible relevant damage mechanisms in the LG window components, while size effects for target LG windows are also addressed under a multitude of blast loading configurations.

Keywords: blast; damage; failure; glass windows; near-field; numerical modelling

1. Introduction

The quantification and determination of the blast protection levels attained by glass windows and facades is of crucial importance for both safety and security design purposes (Bedon *et al.* 2018a), and it is normally performed through experimental tests or coupled experimental-numerical investigations (Kranzer *et al.* 2005, Larcher *et al.* 2012, Spiller *et al.* 2016, Chen *et al.* 2021). In the recent years, it is commonly accepted that numerical methods have become much

*Corresponding author, Associate Professor, E-mail: chiara.bedon@dia.units.it

^aScientific and Technical Project Officer, E-mail: damijan.markovic@ec.europa.eu

^bScientific and Technical Project Officer, E-mail: vasilios.karlos@ec.europa.eu

^cScientific and Technical Project Officer, E-mail: martin.larcher@ec.europa.eu

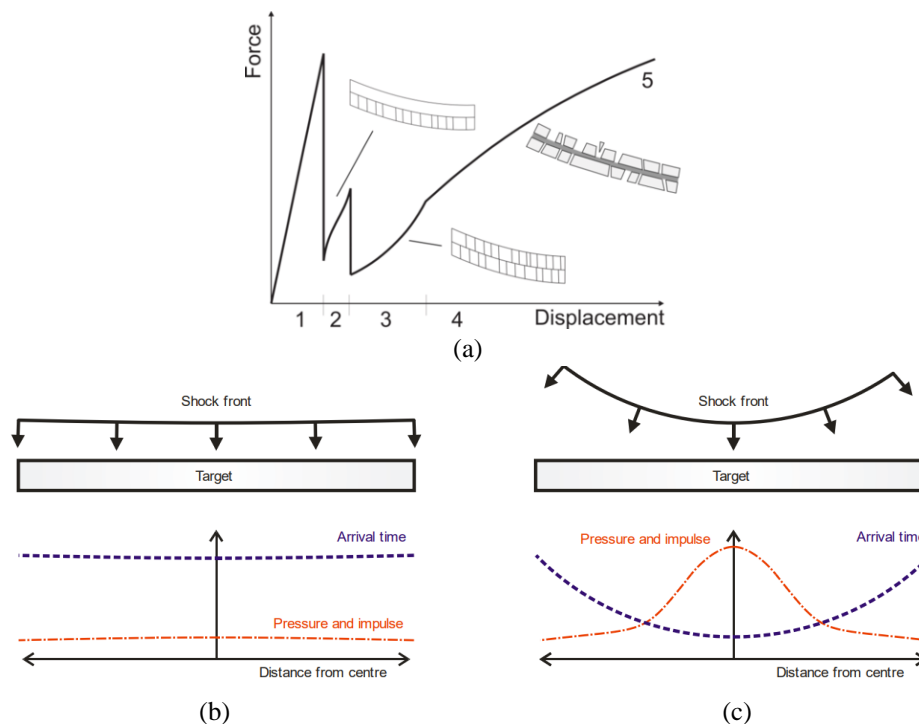


Fig. 1 (a) Schematic force-displacement behaviour of a double laminated glass panel in elastic and post-breakage stages and (b)-(c) typical blast interaction diagram and loading parameters associated with (b) far-field and (c) near-field blast loading (reproduced from Rigby *et al.* 2014)

more powerful and efficient with respect to this kind of applications (Larcher *et al.* 2016). For the analysis of laminated glass (LG) components and systems under blast loading, these methods proved to be effective, thanks to appropriate validation with experiments. Examples can be found for various LG panels and framed glass systems (Larcher *et al.* 2012, Larcher *et al.* 2016, Spiller *et al.* 2016, Pelfrene *et al.* 2016), or even triple insulated glass units (Sielicki *et al.* 2020, Bedon *et al.* 2022), and up to complex façade systems under blast (Deng and Jin, 2010, Amadio and Bedon, 2012, Santos *et al.* 2016, Marchand *et al.* 2017) or even building systems with glass façades (Bedon and Amadio 2018). The common characteristic of these numerical studies is that even complex damage mechanisms and kinematic interactions are taken into account for constitutive materials to reproduce progressive damage and collapse of the window components.

Among others, the typical post-fracture response of a laminated glass panel is particularly challenging (Fig. 1(a)), and for a given window/façade it is typically complex to predict, due to its strict sensitivity to a multitude of coupling interactions among the involved components (i.e., intact glass, glass fragments, bonding interlayer, fixing systems, etc.). Moreover, most of literature studies are mostly referred to medium- or even far-field blast loading only, especially for glass systems. A careful attention is thus required for near-field blast configurations (Figs. 1 (b)-(c)), given that they are associated to well-known specific phenomena compared to far-field (Rigby *et al.* 2014), which are by the moment mostly addressed for non-glazed building components (Dua and Braimah 2016). Near field configurations are in particular important in order to design protection against the threat of drones equipped with explosive (small charges, small distance).

Table 1 Summary of examined LG windows under near-field blast, with 6+6 mm thick glass layers and 2.28 mm thick PVB bonding. *= for 1/4th of the nominal geometry (Section 2.2)

Window system	B [m]	H [m]	Mesh elements *	DOFs *
LGW-1	1.09	0.89	≈ 34,000	≈ 205,000
LGW-2	1.2	1.5	≈ 45,000	≈ 275,000
LGW-3	1.5	3	≈ 115,000	≈ 690,000

Starting from the consideration that glass material is highly vulnerable to blast loading (Zhang *et al.* 2013, Zhang and Bedon 2017), special attention should be thus spent for the analysis of typical performances and expected safety levels.

In this paper, the attention is given to extensive FE numerical parametric analyses on laminated glass window^a targets under near-field blast loading. The performance of different typical laminated glass panels in use for windows and facades, when exposed to near-field blast, is explored. Parametric numerical analyses are presented to highlight the differences in the behaviour and the failure mechanism of laminated glass under near-field explosions, in particular in comparison to far-field explosions.

2. Numerical analysis

2.1 Reference configurations and loading

The presently reported investigation is carried out with the support of FE numerical models developed in ABAQUS/Explicit (Simulia).

For the parametric analysis of LG panes under near-field blast, different configurations are also taken into account (Table 1). For all of them, the LG composition was set to 6 mm thick glass layers and a 2.28 mm bonding of Poly Vinyl Butyral (PVB). Boundaries, mechanical interactions and material properties were calibrated as in Sections 2.2. and 2.3.

In terms of loading configurations, through the parametric numerical analysis, the investigation included multiple blast scenarios for LGW-1, LGW-2 and LGW-3 target systems, in order to facilitate a generalized analysis of performance indicators and failure phenomena. In particular, the attention in loading setup was given to various configurations of interest for the capacity assessment of glass windows under blast (Larcher *et al.* 2016). The study included especially variations of blast input parameters in terms of equivalent charge W of Trinitrotoluene (TNT, in kg) and detonation distance R from the target surface (i.e., the distance from the explosion source to the loaded point, in m), and thus resulting in a sufficiently wide range of corresponding stand-off distances (in $\text{m}/\text{kg}^{1/3}$)

$$Z = \frac{R}{\sqrt[3]{W}} \quad (1)$$

^a The term window is here used even if the testing assumes a very rigid window frame as it might be seldom find in real applications.

Based on parametric modification of W and R input data, the so-calculated Z parameter was modified in the range of 0.5 minimum and 7.5 maximum.

From a numerical point of view, the typical FE simulation included two specific loading contributions and stages. The first one was defined to be representative of precompression / clamping force distributed at the edge restraints (steel plates), and was kept constant during the blast loading stage. In this manner, the experimental setup as required in European Standard EN 13541 2012 was properly taken into account for the blast simulations (Larcher *et al.* 2012). The second stage and loading contribution was defined to represent near-field blast term, which included detonation, arrival time, wave impact and analysis of the dynamic response for each target LG window. In terms of explosion, among various formulations for the blast wave modelling of structural components (Karlos and Solomos 2013, Karlos *et al.* 2016, Figuli *et al.* 2020, Catovic and Kljuno 2021), the present investigation was based on the “CONWEP” (conventional weapons effects blast loading model) fluid interaction from ABAQUS library, which follows the Kingery-Bulmash polynomial expression for pressure time history from (Kingery and Bulmash 1984). More precisely, high-order polynomial equation functions are taken into account, using regression analysis, based on the original test data reported in (Kingery and Bulmash 1984, Hyde 1988). Various blast wave propagations can be hence efficiently simulated by setting the coordinates of detonation point R , the explosive charge W .

2.2 Geometry and material properties

To ensure high accuracy of non-linear dynamic simulation estimates, the reference FE model was described in the form of full three-dimensional (3D) composite assembly, with detailed description of layered section composition, boundaries, loading setup and possible damage initiation and propagation for the constituent materials in use. Due to symmetry considerations, $1/4^{\text{th}}$ of the nominal geometry was taken into account in parametric simulations, with appropriate boundary conditions at the symmetry planes (Fig. 2(a) and Table 1).

During the blast loading stage, the dynamic response of the system was addressed especially in terms of deflection in the centre of the glass (P1 control point in Fig. 2(a)). Major attention was also given to reaction forces in supports, as well as possible occurrence and magnitude of damage phenomena in all components, ranging from crack initiation up to collapse of the system.

To note that the LG section for the reference glass window was assumed rigidly restrained along the edges (EN 13541 2012). For FE modelling purposes, this specific boundary condition was geometrically and mechanically reproduced by introducing the LG panel section in two rubber layers and additional steel clamping plates as in Fig. 2(a). For the same reason, an initial uniform precompression force/clamping pressure corresponding to 14 N/cm^2 was also taken into account in the numerical simulations (EN 13541 2012).

A special attention was then given to material characterization. To this aim, glass was numerically described in ABAQUS with a “brittle cracking” constitutive law, where input parameters can be specified in terms of elastic modulus and fracture parameters for tensile breakage and post-cracking stage. In doing so, the “erosion” option was taken into account for propagation of cracks in glass layers. More precisely, the “brittle cracking” material model assumes a Rankine failure criterion for the first crack detection in the brittle materials. For the present investigation, glass material was thus assumed to behave linear elastically until the exceedance of the assigned tensile strength f_t by the maximum principal tensile stress. To note that for similar modelling assumptions, although crack detection is based purely on Mode I fracture

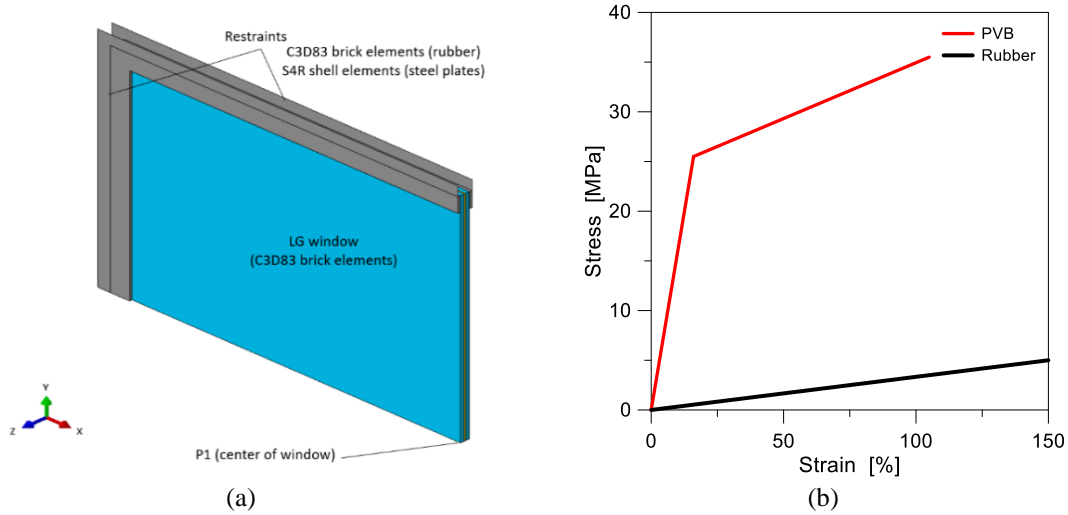


Fig. 2 (a) Model assembly (1/4th the nominal geometry of window) and (b) input material properties for PVB and rubber (ABAQUS)

considerations, the simulated post-cracked behaviour includes both Mode I (tension softening/stiffening) and Mode II (shear softening/retention) phenomena.

Being a “smeared” model, the brittle cracking option, moreover, does not track individual macro cracks, but the presence of cracks—having surface of propagation perpendicular to the direction of maximum principal stresses—is usually taken into account in the constitutive calculations performed at each material point, in the form of stress and stiffness degradation. Input parameters of this damage model are thus not only the tensile strength of glass f_t but also its fracture energy, which was preliminary set equal to $G_f=3 \text{ J/m}^2$ (Haldimann *et al.* 2008, Bedon and Louter 2014). To note that such an input fracture energy is responsible of Mode I phenomena.

To account for possible Mode II phenomena, the post-cracked behaviour was also described by means of the intrinsic “brittle shear” sub-option of “brittle cracking” material model in ABAQUS. Based on the adopted shear retention model, more in detail, the cracked shear modulus of glass ($G_{glass,c}$) was estimated in each simulation as a fraction of the uncracked shear modulus G_{glass} , that is

$$G_{glass,c} = \beta(\varepsilon_{nn}^{ck}) \cdot G_{glass} \quad (2)$$

For the variable shear retention factor β in Eq. (2), which has a non-constant value dependent on the crack opening strain ε_{nn}^{ck} (with $\beta_{max}=1$ before crack initiation and $\beta_{max}=0$ at the complete loss of aggregate interlock), an exponential law was used

$$\beta(\varepsilon_{nn}^{ck}) = \left(1 - \frac{\varepsilon_{nn}^{ck}}{\varepsilon_{max}^{ck}}\right)^p \quad (3)$$

with ε_{max}^{ck} representing the ultimate crack opening strain. The material parameter p , based on earlier literature calibration (see for example (Bedon and Louter 2014)), was assumed equal to $p=5$.

In any case, it has also to be noted that the main advantage of the adopted material model for

the present investigation is given by the physical detection of damage and by the additional deletion from the mesh (with erosion) of cracked elements. To ensure the convergence of simulations after glass cracking, thus to avoid excessive distortion in the damaged elements, the “brittle failure” sub-option was in fact taken into account in the parametric simulations. In doing so, the critical displacement u_{ck} , corresponding to cracked element erosion from the mesh, was estimated as

$$u_{ck} = \frac{2G_f}{f_t} \quad (4)$$

The presently assumed mechanical parameters for glass generally resulted, as highlighted by comparative analysis of parametric results, in almost immediate deletion of cracked elements at the first exceeding of the tensile strength. In ABAQUS “brittle cracking” model, crack closing and reopening may in fact also take place along the directions of the crack surface normal, but this could happen only when the stress becomes compressive, which is no interest for present study, where the imposed loading induces exclusively monotonously increasing strains.

For the bonding PVB foils, an elastic-plastic with hardening constitutive model was used (equivalent Von Mises constitutive law), with input properties derived from (Zhang *et al.* 2013), see Fig. 2(b). In addition to conventional modelling approaches of literature for structural glass applications, the “ductile damage” material option was also taken into account, to facilitate possible tearing of the interlayer in the post-yielding stage, once the ultimate stress-strain capacity in Fig. 2(b) is first achieved. To this aim, damage parameters were again derived from the experimental material characterization reported in (Zhang *et al.* 2013).

Rubber pad layers for the supports along the edges (i.e., interposed to steel fixing plates and the typical LG window) were characterized by linear elastic behaviour (Fig. 2(b)), where the input mechanical properties were calibrated as in (Larcher *et al.* 2012, Larcher *et al.* 2016). Finally, for the steel plates present at edge restraints, a linear elastic behaviour was taken into account (Larcher *et al.* 2016).

2.3 Mesh and interactions

In terms of mesh, full three-dimensional solid assemblies were described in ABAQUS, to reproduce the reference LG section of windows like in Table 1 and all the restraint components. Based on a preliminary mesh sensitivity analysis, the reference mesh pattern for the LG panel system was described with a roughly unsymmetrical scheme. The minimum size was set in 1.5 mm (i.e., close to the window centre), with a maximum size of 8÷10 mm for brick elements, especially in the region of edge restraints (Fig. 3(a)). To note that the mesh scheme was set as regular along the edge restraints of target windows. The transition from minimum-to-maximum edge seeds was satisfied by free meshing techniques available in ABAQUS. Based on preliminary sensitivity studies, moreover, a single mesh element was taken into account along the thickness of each glass layer and PVB.

Overall, the use of irregular mesh schemes for glass and PVB layers resulted in a combination of a majority of 8-node brick elements (C3D8 type) and a minimum number of 6-node wedge elements (C3D6) from ABAQUS library. Both C3D8 and C3D6 options represent general purpose, linear solid elements characterized by full-integration.

In terms of mechanical interactions for the LG window components (Fig. 3(b)), a special attention was given to the analysis and realistic description of possible damage phenomena of

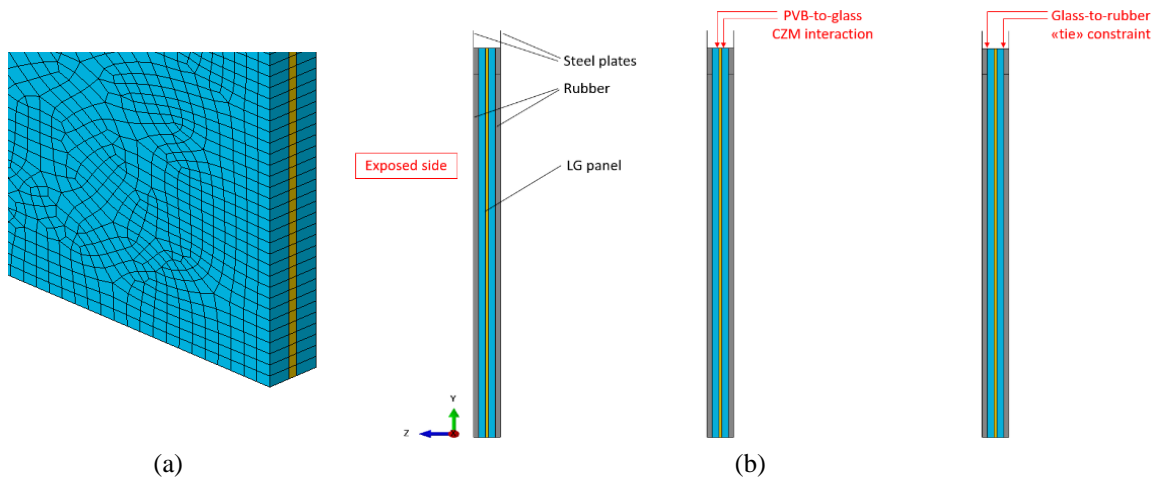


Fig. 3 (a) Mesh detail and (b) mechanical interactions for the reference setup, with cross-sectional view of 1/4th the nominal geometry of window (ABAQUS)

interest. To this aim, a rigid surface bond (“tie” constraint) was assigned at the interface of rubber pads and steel clamping plates, all along the edges of the examined systems. Similarly, the mechanical interaction for the LG-to-rubber interface was reproduced with a rigid “tie” constraint. In this manner, possible local deformations in the region of restraints for the LG window under blast were taken into account in terms of flexibility of rubber pads, or even damage in glass-PVB components (Section 2.2).

A key role was indeed assigned to the PVB-to-glass interface, where complex damage phenomena can take place (Larcher *et al.* 2012, Gao *et al.* 2017). To this aim, a Cohesive Zone Modelling (CZM) technique was used and a CZM-based surface interaction was introduced to facilitate possible delamination of PVB and glass layers (Bedon *et al.* 2018b). To this aim, input mechanical properties were described in terms of initial stiffness parameters for the involved surfaces (based on default option) and ultimate strength values for possible PVB delamination (based on material characterization as in Section 2.2). To note that “repeated contacts” were also possibly taken into account in the characterization of CZM surface interaction for glass-PVB interfaces. This last option was used to avoid any possible passing through of the glass-PVB elements in the post-fracture stage, i.e., in case a new contact is established between them (especially for those elements previously involved in the original cohesive contact and fully debonded).

2.4 Preliminary validation to experiments

Validation of FE modelling strategy was carried out towards the blast response of selected literature experimental samples. In doing so, both LG specimens under far-field and near-field explosions were taken into account.

In the first case, the LG window explored in (Kranzer *et al.* 2005) was numerically investigated. The sample consists of a $t_{tot}=7.5$ mm thick double LG section, composed of 3 mm thick float glass layers and 1.52 mm PVB bonding. The LG sample (0.9 m×1.1 m its size) was subjected to various pentaerythritol tetranitrate (PETN) charges (with $W=0.125$ kg, 0.25 kg and 0.5

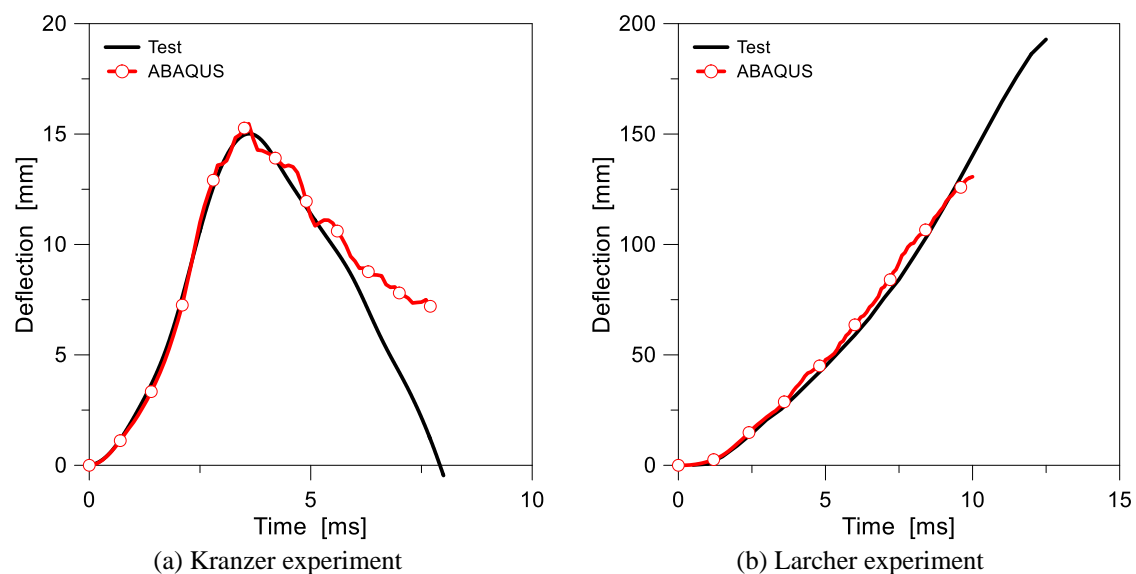


Fig. 4 Validation of modelling strategy and calibration towards literature experiments (ABAQUS)

kg) and detonation distances ($R=2$ m, 3.7 m and 5.75 m). The original experimental setup was designed to reproduce a stand-off distance Z equal to 4, 6 and 7 m/kg^{1/3} respectively. For the present comparative analyses, the charge $W=0.125$ kg at a distance $R=2$ m was primarily taken into account, which corresponds for the experimental discussion reported in (Kranzer *et al.* 2005) to the “4-FX014 Q=0.125 kg JE Test” experimental setup and results.

The corresponding numerical deflection from present analysis carried out in ABAQUS is proposed in Fig. 4(a) with the red thick curve, where it can be noted a rather good correlation with the original test results reproduced from (Kranzer *et al.* 2005).

A second validation was carried out towards the experiments presented in (Larcher *et al.* 2012), and carried out on LG windows with similar conventional size ($H=0.89$ m \times $B=1.09$ m), but a relatively thick LG panel composition ($t_g=6$ mm for the two glass layers and $t_{int}=2.28$ mm for the bonding PVB). Results in Fig. 4(b) show also in this case a good agreement between the present FE numerical analysis and the experimental trends of deflections at the centre of the window. To note that both in the experimental setup from (Larcher *et al.* 2012) and in the present numerical analysis, collapse of target LG sample resulted from propagation of minor glass cracks in the two glass layers and subsequent sudden propagation of a major tearing failure in the PVB bonding film, with final collapse of the LG window.

3. Parametric numerical analysis

3.1 Key performance indicators

The analysis of FE numerical results was focused on a selection of performance indicators to quantify the load-bearing capacity of windows under near-field blast loading. In doing so, for a given blast scenario, the attention was focused on the analysis of:

Table 2 Classification of window response for the present parametric numerical analysis

Window response	Associated phenomena	Safety level
Elastic	Linear elastic status of glass, interlayer/ supports elastic (minor cracks in glass allowed)	High
Initial damage	First crack in glass and local rupture of the interlayer	Moderate
Minor damage	Propagation of glass cracks and interlayer rupture to more than one region of the window, possible localized damage in the supporting components and restraints	Limited
Major damage/ Near collapse	Severe damage in various regions of glass, interlayer/supports and incipient collapse of the window (no residual load-bearing capacity)	Unsafe

- Deflection at the centre of windows,
- Maximum velocity at the centre of windows,
- Reaction forces at the boundaries,
- Detection of minimum charge W_{\min} in near-field conditions to generate first damage (cracks) in glass and rupture of interlayer,
- Damage evolution in glass and interlayers, with fall-out of window,
- Possible damage in restraints (soft rubber layers),
- Residual load-bearing capacity (i.e., momentum of the composite system),
- Type of failure mechanism (if any).

The performance of each LG window under blast was numerically classified as proposed in Table 2. From a practical point of view, it is however to note that once W_{\min} is calculated iteratively for an imposed R , the corresponding numerical results can be further efficiently quantified in terms of “minimum stand-off distance” for load-bearing capacity assessment, Z_{fail} , where $W_{\min}=W$ in Eq. (1). In this regard, it is to remind that that the assessment of the different failure behaviours is sometimes not very strict. Also, the difference in terms of input loading parameters between the different response types classification might be small.

3.2 Determination of load-bearing capacity

For design applications, disregarding possible qualitative aspects from the discussion of parametric numerical results, a key characteristic is the information regarding the load-bearing capacity for a given window under assigned blast loads.

Part of FE investigation was focused on the detection and quantification of load-bearing capacity of LGW-1, LGW-2 and LGW-3 systems, that is the minimum charge W (W_{\min}) that a target LG window could resist for an assigned detonation distance R , with evidence of first glass cracking and rupture of PVB interlayer, that is a minimum “initial damage” defined as in Table 2.

Such a study required the performance of an extensive number of FE simulations, in which-for a fixed R -the input charge W was iteratively modified to find the “initial damage” configuration (Fig. 5). This means that, for a given detonation distance R , the same window was repeatedly subjected to different tentative charges W , which were progressively increased or decreased to detect the minimum charge value (W_{\min}) leading to the first initial damage initiation in the LG window.

To note that in Step (3) of Fig. 5, the accuracy of numerical derivations for “Initial damage” condition was ensured by extensive iterations in terms of assigned charge W . Due to the imposed

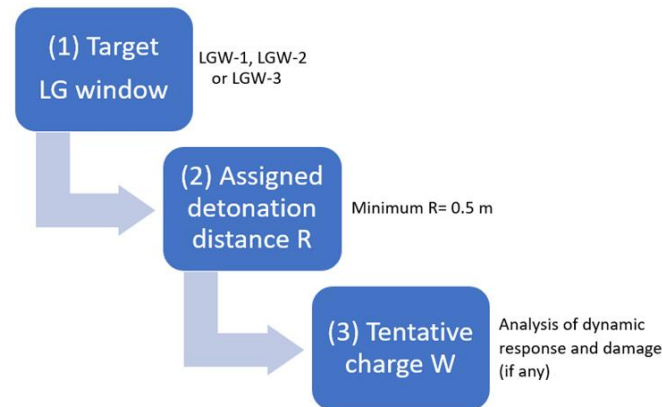


Fig. 5 Flowchart for the determination of load-bearing capacity in the parametric study

detonation distances R (in the range of 0.5 m and up to 10 m), the tentative initial charge W was generally set in $W_0=10$ kg and then progressively modified, as a function of observed dynamic responses as in Table 2.

In each simulation, close to the transition of “Elastic” and “Initial damage” responses for a given LG window, the incremental modification $\Delta W(\pm)$ for iterations in terms of W was set in accuracy levels denoted by:

- $\Delta W = \pm 1$ kg, for detonation distances R higher than 2 m,
- $\Delta W = \pm 0.5$ kg, for detonation distances R comprised between 1 m and 2 m,
- $\Delta W = \pm 0.05$ kg, for detonation distances R comprised between 0.5 m and 1 m.

3.3 Performance assessment

The typical FE numerical analysis was mostly affected by computational cost associated to mesh refinement and constitutive damage laws for materials in use, rather than total duration of positive phase t_d for the input blast wave.

A typical example is reported in Fig. 6 for the LGW-1 system, when investigated under the effects of explosive event with $R=1$ m and $W=5$ kg.

While the presented R - W configuration was found associated-according to Table 2-to “major damage / collapse” for the LGW-1 system, it is worth to note in Fig. 6 the relatively short duration of blast loading stage, which was typically measured in the order of ≈ 1 ms for most of the examined configurations.

The structural effect of near-field blast phenomenon can be also clearly noted from contour plots reported in Fig. 6. From the selected time instants, it can be seen the rapid and non-uniform evolution of blast pressure due to near-field setup. The first damage in glass and PVB generates after around 1.5 ms and the residual bending capacity of LG window rapidly decreases, as also notable by the mostly linear increase of deflections in P1 control point. After 3.5 ms, a major part of LG window is fully detached from the edges and frame, leading to collapse of the system.

3.5 Load-bearing capacity and window size effect

The parametric investigation of this section emphasizes the expected load-bearing capacity as a

function of size effect for the examined systems under various blast loading conditions. To this aim, the calculation process to detect W_{min} and Z_{fail} was carried out in accordance with Fig. 5.

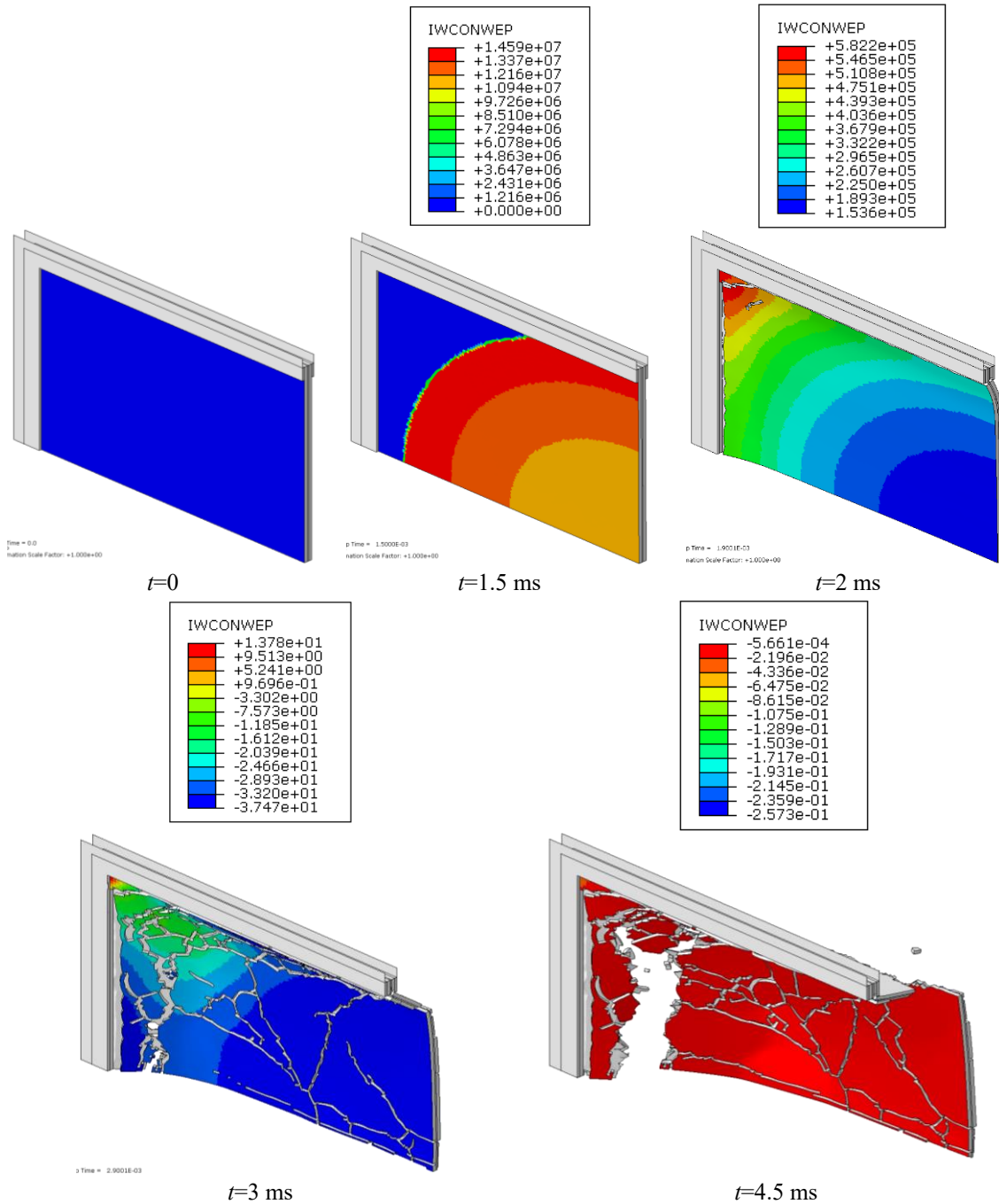


Fig. 6 Selected contour plots (axonometric front view) of input pressure evolution for LGW-1 system under $R=1$ m and $W=5$ kg of explosive charges (ABAQUS). Pressure legend in Pa

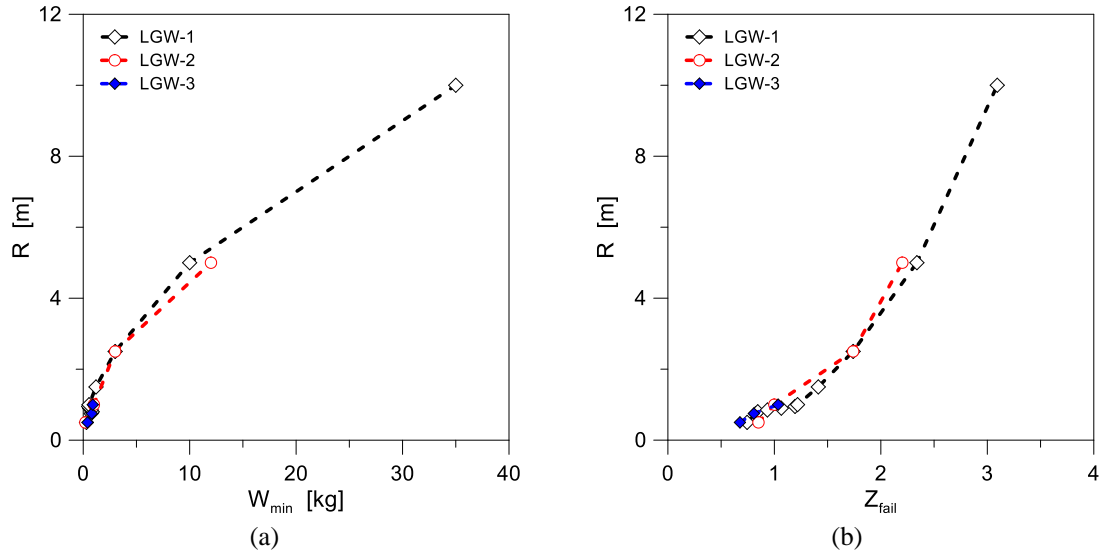


Fig. 7 Load-bearing capacity for the examined LGW-1, LGW-2 and LGW-3 systems under various W-R combinations of explosive charges W and detonation distances R : in evidence, the (a) minimum charge W_{min} or (b) corresponding stand-off distance Z_{fail} , for a given R value (ABAQUS)

Both R - W_{min} and R - Z_{fail} parametric results are shown in Fig. 7, for windows LGW-1, LGW-2 and LGW-3. It is worth to note that through the parametric study the detonation distance R is changed in the range between 0.5 m to 10 m, and iterative simulations are carried out at each assigned value of R to minimize W , as a function of the observed damage.

From the comparative results in Fig. 7, in terms of numerical estimates, it is interesting to see a rather close agreement in the shape and amplitude of numerical curves, for separate LGW systems. This suggests, for a given cross-section layout and thickness, that size effects have only a minor effect on the load-bearing capacity of the examined systems, at least from a theoretical point of view. A major modification for the numerical plots in Fig. 7, as a function of LG window size, can be noted for near-field configurations characterized by $R < 1$ m. These blast configurations are associated to rather localized damage mechanisms, due to spherical blast wave propagation, and the size effect can involve minimum modifications in load-bearing performance and capacity of the examined systems. Finally, it is also worth to note that for all the examined systems, near-field configurations are associated to very small W_{min} charge estimates.

Among others, the maximum velocity at the centre of a target window is well representative of its mechanical features, on one side, and features of the input blast pressure, on the other side. As such, the velocity parameter can be used as both a quantitative and qualitative result to compare LG systems which are qualitatively similar but characterized by modifications in their geometrical (and thus mechanical) features. In Fig. 8, typical comparisons are proposed for LGW-1, LGW-2 and LGW-3 systems in terms of maximum velocity measured at the centre of the target LG panel, for a given detonation distance R , when the first crack initiation and interlayer rupture manifests in the system, that is for W_{min} (or Z_{fail}). In confirmation of previous qualitative comparative results, it is thus worth to note in Fig. 8 that the maximum velocity at failure (v_{fail}) for the examined systems is slightly sensitive to the size of target LG panels, when the first failure manifests, but mostly depends on the thickness of constitutive layers for the resisting cross-section. Additionally,

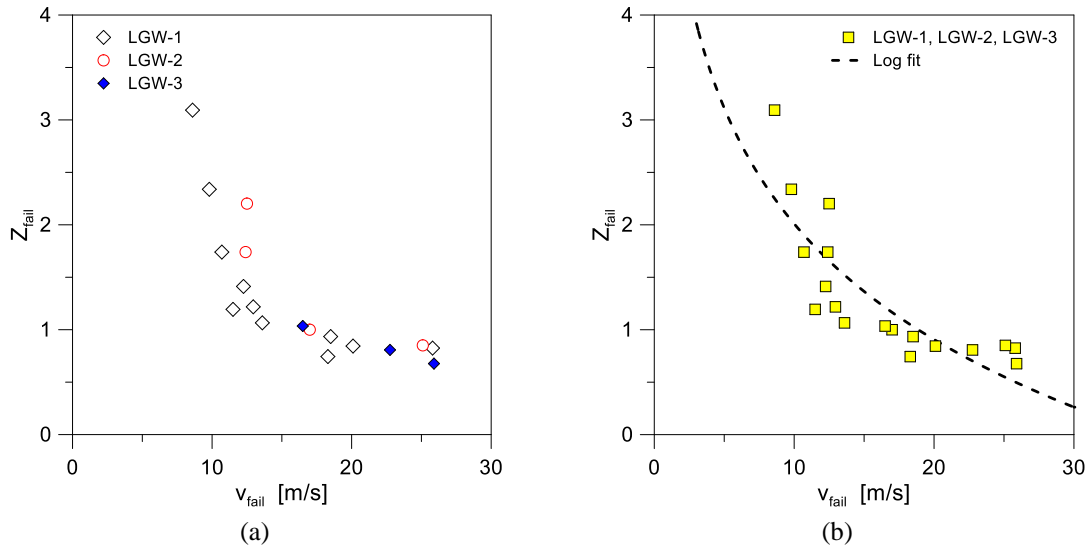


Fig. 8 Evolution of maximum velocity at failure, v_{fail} , as a function of minimum stand-off distance Z_{fail} for systems LGW-1, LGW-2 and LGW-3 (ABAQUS): (a) individual windows and (b) fitting curve

parametric numerical results for the examined windows can be rather accurately fitted by

$$Z_{fail} = 26.15v_{fail}^{-1.13} \quad (5)$$

with $R^2=0.75$ the coefficient of correlation calculated from Eq. (5) for the present numerical results. This also suggests a rather limited influence of size and aspect ratio effects, compared to the cross-sectional features of target windows.

4. Conclusions

The determination of the blast protection level and minimum load-bearing capacity for a laminated glass (LG) windows or façade component is of crucial importance for safety design purposes. In most of cases, such an operation is carried out based on complex experimental analysis and often by the support of Finite Element (FE) numerical models.

In recent years, FE numerical methods have become much more powerful, and several literature applications can be found for LG systems under medium/far-field blast loading. Differing from major literature outcomes, this present study focused on the performance assessment and structural behaviour of LG windows under near filed blast loading.

From the parametric analysis, it was shown that:

- Under near-field, LG windows can be highly vulnerable to even small charges. Special attention is thus required for mitigation and design,
- The size and aspect ratio of LG windows under near-field blast has apparently minor effect on the minimum load-bearing capacity. However, further geometrical and loading configurations should be taken into account,
- Overall, next studies will be carried out to further quantify and explore the effect of cross-sectional features (like for example the thickness of constitutive layers) as well as boundaries

on the actual dynamic response and load-bearing capacity of target LG windows and façade components under near-field blast.

Acknowledgments

The research described in this paper was financially supported by the European Commission-Joint Research Centre.

References

- Amadio, C. and Bedon, C. (2012), “Viscoelastic spider connectors for the mitigation of cable-supported façades subjected to air blast loading”, *Eng. Struct.*, **42**, 190-200. <https://doi.org/10.1016/j.engstruct.2012.04.023>.
- Bedon, C. and Amadio, C. (2018), “Numerical assessment of vibration control systems for multi-hazard design and mitigation of glass curtain walls”, *J. Build. Eng.*, **15**, 1-13. <https://doi.org/10.1016/j.jobe.2017.11.004>.
- Bedon, C. and Louter, C. (2014), “Exploratory numerical analysis of SG-laminated reinforced glass beam experiments”, *Eng. Struct.*, **75**, 457-468. <https://doi.org/10.1016/j.engstruct.2014.06.022>.
- Bedon, C., Larcher, M., Bez, A. and Amadio, C. (2022), “Numerical analysis of TGU windows under Blast-GLASS-SHARD outlook”, *Proceedings of Challenging Glass*, Ghent, Belgium, June.
- Bedon, C., Machalická, K., Eliášová, M. and Vokáč, M. (2018b), “Numerical modelling of adhesive connections including cohesive damage”, *Challenging Glass Conference Proceedings*, **6**, <https://doi.org/10.7480/cgc.6.2155>.
- Bedon, C., Zhang, X., Santos, F., Honfi, D., Kozłowski, M., Arrigoni, M., Figuli, L. and Lange, D. (2018a), “Performance of structural glass facades under extreme loads—design methods, existing research, current issues and trends”, *Constr. Build. Mater.*, **163**, 921-937. <https://doi.org/10.1016/j.conbuildmat.2017.12.153>.
- Catovic, A. and Kljuno, E. (2021), “Comparison of analytical models and review of numerical simulation method for blast wave overpressure estimation after the explosion”, *Adv. Sci., Technol. Eng. Syst. J.*, **6**(1), 748-756. <https://doi.org/10.25046/aj060182>.
- Chen, X., Chen, S. and Li, G.Q. (2021), “Experimental investigation on the blast resistance of framed PVB-laminated glass”, *Int. J. Impact Eng.*, **149**, 103788. <https://doi.org/10.1016/j.ijimpeng.2020.103788>.
- Deng, R. and Jin, X. (2010), “Numerical simulation for blast analysis of insulating glass in a curtain wall”, *Int. J. Comput. Meth. Eng. Sci. Mech.*, **11**(3), 162-171. <https://doi.org/10.1080/15502281003702302>.
- Dua, A. and Braimah, A. (2016), “State-of-the-art in near-field and contact explosion effects on reinforced concrete columns”, *Proceedings of Resilient Infrastructure*, London, UK.
- EN 13541 (2012), Glass in Building-Security Glazing-Testing and Classification of Resistance Against Explosion Pressure, European Committee for Standardization (CEN), Brussels, Belgium.
- Figuli, L., Cekerevac, D., Bedon, C. and Leitner, B. (2020), “Numerical analysis of the blast wave propagation due to various explosive charges”, *Adv. Civil Eng.*, **2020**, Article ID 8871412. <https://doi.org/10.1155/2020/8871412>.
- Gao, W., Xiang, J., Chen, S., Yin, S., Zang, M. and Zheng, X. (2017), “Intrinsic cohesive modeling of impact fracture behavior of laminated glass”, *Mater. Des.*, **127**, 321-325. <https://doi.org/10.1016/j.matdes.2017.04.059>.
- Haldimann, M., Luible, A. and Overend, M. (2008), “Structural use of glass”, *IABSE*, Zurich, Switzerland.
- Hyde, D. (1999), *Users' Guide for Microcomputer Programs CONWEP and FUNPRO-Applications of TM 5-885-1*, U.S. Army Engineer Waterways Experimental Station, Vicksburg, VA.

- Karlos, V., Solomos, G. and Larcher, M. (2016), "Analysis of blast parameters in the near-field for spherical free-air explosions", JRC Technical Report, EUR 27823, Publications Office of the European Union, Luxembourg.
- Kingery, C. and Bulmash, G. (1984), "Air blast parameters from TNT spherical air burst and hemispherical burst", Technical report ARBRL-TR-02555, AD-B082 713, U.S. Army Ballistic Research Laboratory, Aberdeen Proving Ground, MD Ballistic Research Laboratories.
- Kranzer, C., Gürke, G. and Mayrhofer, C. (2005), "Testing of bomb resistant glazing systems. Experimental investigation of the time dependent deflection of blast loaded 7.5 mm laminated glass", *Proceedings of the Glass Processing Days*, Tampere.
- Larcher, M., Arrigoni, M., Bedon, C., van Doormaal, J.C.A.M., Haberacker, C., Hüsken, G., Millon, O., Saarenheimo, A., Solomos, G., Thamie, L., Valsamos, G., Williams, A. and Stolz, A. (2016), "Design of blast-loaded glazing windows and facades: A review of essential requirements towards standardization", *Adv. Civil Eng.*, **2016**, Article ID 2604232. <https://doi.org/10.1155/2016/2604232>.
- Larcher, M., Solomos, G., Casadei, F. and Gebbeken, N. (2012), "Experimental and numerical investigations of laminated glass subjected to blast loading", *Int. J. Impact Eng.*, **39**, 42-50. <https://doi.org/10.1016/j.ijimpeng.2011.09.006>.
- Marchand, K., Davis, C., Sammarco, E., Buy, J. and Casper, J. (2017), "Coupled glass and structure response of conventional curtain walls subjected to blast loads: validation tests and analysis", *Glass Struct. Eng.*, **2**, 17-43. <https://doi.org/10.1007/s40940-016-0037-y>.
- Pelfrene, J., Kuntsche, J., Van Dam, S., Van Paepegem, W., Schneider, J. (2016), "Critical assessment of the post-breakage performance of blast loaded laminated glazing: Experiments and simulations", *Int. J. Impact Eng.*, **88**, 61-71. <https://doi.org/10.1016/j.ijimpeng.2015.09.008>.
- Rigby, S.E., Tyas, A., Clarke, S.D., Fay, S.D., Warren, J.A., Elgy, I. and Gant, M. (2014), "Testing apparatus for the spatial and temporal pressure measurements from near-field free air explosions", *Proceedings of the 6th International Conference on Protection of Structures against Hazards*, Tianjin, China.
- Santos, F., Cismasiu, C. and Bedon, C. (2016), "Smart glazed cable facade subjected to a blast loading", *Struct. Build.*, **169**(3), 223-232. <https://doi.org/10.1680/jstbu.14.00057>.
- Sielicki, P.W., Bedon, C. and Zhang, X. (2020), "Performance of TGU Windows under Explosive Loading", *Soft Target Protection. NATO Science for Peace and Security Series C: Environmental Security*. Springer, Dordrecht, Hofreiter.
- Simulia, ABAQUS Computer Software, V. 6.14, Dassault Systèmes, Providence, RI, USA.
- Spiller, K., Packer, J.A., Seica, M.V. and Yankelevsky, D.Z. (2016), "Prediction of annealed glass window response to blast loading", *Int. J. Impact Eng.*, **88**, 189-200. <https://doi.org/10.1016/j.ijimpeng.2015.10.010>.
- Zhang, X. and Bedon, C. (2017), "Vulnerability and protection of glass windows and facades under blast: Experiments, methods and current trends", *Int. J. Struct. Glass Adv. Mater. Res.*, **1**(2), 10-23. <https://doi.org/10.3844/sgamrsp.2017.10.23>.
- Zhang, X., Hao, H. and Ma, G. (2013), "Parametric study of laminated glass window response to blast loads", *Eng. Struct.*, **56**, 1707-1717. <https://doi.org/10.1016/j.engstruct.2013.08.007>.